npj | vaccines

Article

Published in partnership with the Sealy Institute for Vaccine Sciences

https://doi.org/10.1038/s41541-025-01359-8

Development of a J paramyxovirus-based vaccine vector

Elizabeth R. Wrobel[1], Julia Paton-Smith[1], Caroline Piotrowski[1], Stephen R. Welch[2], Elif Karaaslan[1], Maria Cristina Gingerich[1,3], Aaron Gingerich[1,3], Zhuo Li[3], Jessica R. Spengler[2] & Biao He[1,3] ✉

J paramyxovirus (JPV) is a non-segmented, negative-strand RNA virus in the *Jeilongvirus* genus of the *Paramyxoviridae* family. Recently, a recombinant JPV lacking the small hydrophobic protein (SH) gene (rJPV-ΔSH) has been used as a viral vector for avian influenza virus H5N1 and HIV vaccine development. However, the rJPV-ΔSH vector still causes morbidity and mortality in mice. To further develop this vaccine platform, we generated multiple recombinant JPV (rJPV) mutants and tested their pathogenicity in mice. We found that rJPV lacking the syncytial protein (SP) (rJPV-ΔSP), rJPV with both SH and SP genes deleted (rJPV-ΔSHΔSP) and a JPV lacking coding sequences for SH, SP, and the putative X open reading frame (rJPV-Δ3) were pathogenic in mice. Incorporating mutations in the L gene that mediate pathogenesis into rJPV-Δ3 (rJPV-Δ3-LW-L) resulted in a fully attenuated virus in mice. rJPVΔ3-LW-L-immunized mice were protected during lethal JPV challenge. Furthermore, intranasally administrated rJPV-Δ3-LW-L expressing Nipah virus (NiV) fusion (F) induced anti-NiV-F antibodies in mice and Syrian hamsters, and a single-dose intranasal immunization with rJPV-Δ3-NiV-F-LW-L induced complete protection against lethal NiV challenge in the hamster model. Our work has identified a novel intranasal vaccine vector that is fully attenuated in mice and induces protective immunity in animals.

J Paramyxovirus (JPV) is a member of the *Jeilongvirus* genus in the *Paramyxoviridae* family. It was first isolated from moribund mice with hemorrhagic lung lesions in Australia in 1972[1]. JPV has a negative-sense, single-stranded genome of 18,954 nucleotides that encodes for 8 genes in the order 3'-N-P/V/C-M-F-SH-SP-G-L-5'[2]. Jeilongviruses are unique among paramyxoviruses in that they have 1–2 additional genes that encode accessory proteins, the small hydrophobic protein (SH) and/or the syncytial protein (SP) (previously known as transmembrane protein, TM)[3,4]. All jeilongviruses possess the SP gene, while only some have the SH gene[3]. JPV SH, a type I membrane protein, has been shown to block TNF-α induced apoptosis[5]. A rJPV with SH deletion (rJPV-ΔSH) is attenuated but still induces significant morbidity and mortality in mice[6].The SP of JPV is a type II glycosylated integral membrane protein that promotes cell-to-cell fusion with the JPV fusion (F) protein and the receptor binding protein (G)[7].

A recombinant JPV virus lacking SP (rJPV-ΔSP) is viable and has no growth defect in vitro but is defective in syncytia formation[7]. Cleavage of SP is necessary for its syncytial-promoting activity[4]. JPV also encodes a large open reading frame (termed ORF-X) following the G stop codon, whose corresponding polypeptide has not been confirmed and its function is unknown[8].

There are two strains of JPV: JPV-BH and JPV-LW. JPV-BH is pathogenic in mice, while JPV-LW does not cause any disease in mice[9]. Because of the high sequence identity between JPV-BH and JPV-LW, it is speculated that they are the same viral strain but obtained at different in vitro passages from separate laboratories[9]. There are three amino acid differences in the L gene between the two strains. A rJPV-BH hybrid virus that contains the L gene from the LW strain is completely attenuated in mice, indicating that these sequence differences within the L gene play a critical role in pathogenesis[9].

Nipah virus (NiV) is an emerging zoonotic pathogen that has repeatedly spilled over from bats to humans and livestock with high-case fatality rates across a large geographic range[10]. It is a negative-sense, single-stranded RNA virus in the *Henipavirus* genus of the *Paramyxoviridae* family. NiV was first identified in 1998, when an outbreak of neurological and respiratory disease emerged across pig farms in Malaysia, resulting in 108 human deaths and the culling of over 1 million pigs[11]. Fruit bats in the genus *Pteropus* (flying foxes) are the main reservoir hosts for NiV[11]. In 2001, a geographically distinct NiV strain emerged in India and Bangladesh, where human NiV outbreak events have been reported almost every year

[1]Department of Infectious Diseases, University of Georgia College of Veterinary Medicine, Athens, GA, USA. [2]Viral Special Pathogens Branch, Division of High-Consequence Pathogens and Pathology, Centers for Disease Control and Prevention, Atlanta, GA, USA. [3]CyanVac LLC, Athens, GA, USA. ✉e-mail: bhe@uga.edu

since and are associated with a high mortality rate (60-70%)[12,13]. Spillovers have been linked to the human consumption of contaminated date palm sap and through close contact with domestic animals that have eaten contaminated fruit[14]. NiV spreads between people via close contact with an infected person or their bodily fluids[14]. NiV infection causes a wide array of clinical presentations in people, ranging from asymptomatic infection to acute respiratory infection and fatal encephalitis[15].

There is no licensed vaccine to prevent NiV infection or associated diseases in humans. Most vaccine candidates target the NiV G and/or F protein because they are membrane proteins involved in receptor binding and entry and are readily recognized by the host immune system[13]. Experimental NiV vaccines that have been evaluated in preclinical animal models include recombinant protein[13], mRNA[16], virus-like particles[17], and viral-vectored vaccines[18–23]. While most of these NiV vaccine platforms induce an immune response in laboratory animals, they are typically delivered via intramuscular injection. Although infection of the respiratory tract epithelium majorly contributes to NiV pathogenesis and transmission[24], an intranasal NiV vaccine has not been explored in humans.

Because JPV is a respiratory virus, it is an attractive vector for developing vaccines against pathogens that infect the host through the mucosal surfaces, such as NiV. We recently explored JPV as a vaccine platform for influenza virus H5N1[25]. JPV-SH was replaced with the hemagglutinin (HA) of H5N1 to generate a recombinant JPV expressing HA (rJPV-ΔSH-H5). Mice intranasally immunized with rJPV-ΔSH-H5 were protected from lethal influenza challenge and it was shown to induce strong humoral and cellular responses in rhesus macaques[25]. A rJPV-vectored vaccine against HIV-1 has also been generated by replacing the JPV-SH gene with full-length HIV envelope glycoprotein (rJPV-ΔSH-env) and it induced anti-HIV-gp120 IgG antibodies in mice[26].

A potential issue for using the JPV viral vector system is that the rJPV-ΔSH backbone is not fully attenuated in mice even though rJPV-ΔSH backbone was not pathogenic in non-human primates, and there is no evidence of JPV being pathogenic in humans[25]. One immunization of 4×10^4 PFU rJPV-ΔSH-env in mice resulted in weight loss of 7% at 2 days post-vaccination (dpv)[26]. To reduce pathogenicity of JPV, we generated various mutant JPV viruses and assessed their pathogenicity in mice. We developed a fully attenuated rJPV vector and evaluated the ability of this vector to protect mice from lethal JPV challenge. We then generated a NiV vaccine candidate by inserting the full-length F from the NiV-Malaysia (NiV-M) strain into this backbone, assessed anti-NiV-F humoral responses in mice, and evaluated if a single intranasal immunization could protect against lethal NiV-M challenge in hamsters.

Results

rJPV-ΔSP is pathogenic in a mouse model

An important issue facing the JPV vaccine platform was that the rJPV-ΔSH backbone is not fully attenuated in mice. Unlike other paramyxoviruses, the co-expression of JPV F and G is not sufficient to promote cell-to-cell fusion. For cell-to-cell fusion to occur, the presence of the SP protein along with F or F and G is required[4]. Previously, we generated a recombinant JPV virus lacking SP (rJPV-ΔSP) (Fig. 1A) that is viable and has no growth defects in tissue culture cells but cannot promote syncytium formation[4]. More recently, we reported that cleavage of SP is needed for its syncytial-promoting activity[7]. While the function of SP has been extensively studied in vitro, the impacts of SP deletion on viral pathogenicity in vivo has not been explored.

To examine if the SP deletion results in attenuation, female BALB/c mice were intranasally infected with either 100 µl PBS or 5×10^5 PFU of rJPV or rJPV-ΔSP (n = 5/group) (Fig. 1B). Mice infected with either virus did not exhibit any significant weight loss compared to the PBS mice for the first 5 days post-infection (dpi). At 6 dpi, both virus-infected groups started losing weight. However, the weight loss in rJPV-infected mice was much more pronounced than in the rJPV-ΔSP-infected mice (Fig. 1C). By 9 dpi, all rJPV-infected mice had to be euthanized due to severe weight loss (>20% loss from starting weight for more than 24 hours) and illness (Fig. 1D). At 9 dpi, the rJPV-ΔSP-infected mice had lost approximately 12% body weight, but all survived and recovered to normal body weight by 11 dpi. These results demonstrate the SP deletion only partially attenuates the JPV vector and that rJPV-ΔSP is not a viable vaccine vector.

Deletion of SP and SH together does not result in complete attenuation

The 50% lethal dose (LD_{50}) value for rJPV-ΔSH was previously determined to be 6.7×10^5 PFU compared to 1.76×10^5 PFU for rJPV[6]. Thus, while deletion of SH attenuates the virus, it can still induce significant morbidity and mortality. Consistent with this, mice immunized with rJPV-ΔSH expressing HIV-env still exhibited significant weight loss 2 days post-vaccination[26]. Because deletion of SP also results in partial attenuation in mice (Fig. 1C, D), we generated a virus that has both SH and SP genes deleted (Fig. 2A).

To examine growth kinetics, Vero cells were infected with either rJPV or rJPV-ΔSHΔSP at a multiplicity of infection (MOI) of 0.1. The medium was harvested at 24-hour timepoints and viral titer was determined by plaque assay. rJPV grew to slightly higher titers at 24- and 48-hours post-infection (hpi). However, rJPV-ΔSHΔSP titer exceeded that of rJPV by 4 dpi and maintained a titer over 7 $\log_{10}$ while the rJPV viral titer decreased after its peak (Fig. 2B). Abolishment of SH and SP expression in virus-infected cells was confirmed by Western blot (Fig. 3). Mice (n = 5/group) were intranasally infected with 100 µl PBS or 1×10^6 PFU of rJPV or rJPV-ΔSHΔSP (Fig. 2C). Both virus-infected groups displayed significant weight loss (Fig. 2D). All rJPV-infected mice had succumbed to disease by 4 dpi. While the weight loss was slightly delayed in the rJPV-ΔSHΔSP-infected mice, it was so severe that all mice had to be humanely euthanized by 6 dpi (Fig. 2E). Thus, deletion of SH and SP is not sufficient for complete attenuation.

rJPV-Δ3 is more attenuated than rJPV-ΔSHΔSP in mice, but is still pathogenic

While the function of X is not known, we examined if its deletion would affect pathogenicity in vivo. The rJPV-Δ3 vector was generated by deleting the ORFs for SH, SP, and X (Fig. 4A). Western blotting confirmed that expression of SH and SP protein was abolished in rJPV-Δ3-infected cells (Fig. 3). Because ORF-X does not produce a detectable protein, its deletion was confirmed via RT-PCR (Fig. 4B). rJPV-Δ3 grew to significantly higher viral titers in Vero cells than rJPV at 72, 96, and 120 hpi. (Fig. 4C).

To investigate whether JPV-Δ3 was pathogenic in mice, mice were infected intranasally with 100 µl PBS or 1×10^6 PFU of rJPV or JPV-Δ3 (n = 5/group) (Fig. 4D). All rJPV-infected mice had to be humanely euthanized by 4 dpi due to severe weight loss. The rJPV-Δ3 virus was still pathogenic—by 7 dpi, 3 of the 5 infected mice had to be euthanized due to severe weight loss (Fig. 4E, F). The remaining 2 rJPV-Δ3-infected mice survived and recovered to a normal body weight by 12 dpi. Deletion of X further attenuated the rJPV-ΔSHΔSP vector. However, 60% of the JPV-Δ3-infected mice did not survive, demonstrating that the deletions of SH, SP, and X together are not sufficient to achieve complete attenuation.

Generation of a rJPV-Δ3 backbone with the L gene from a laboratory adapted strain of rJPV

rJPV-Δ3 is still too pathogenic to be used as a vaccine vector in mice. To further attenuate this vector, we generated a rJPV-Δ3 virus that has the L gene from the attenuated JPV-LW strain, which is the critical contributor of its attenuation. There are 2 strains of JPV: JPV-BH and JPV-LW, with the former causing severe disease in mice and the latter causing no signs of illness[9]. JPV-BH has the same genome structure and number of nucleotides as JPV-LW. However, there is one nucleotide difference in the leader sequence and 3 nucleotide differences in the L gene between the two strains. The 3 nucleotide differences in the L gene do change the amino acid residues at those sites (V569I, E590D, D1011E) and replacement of the L gene from JPV-BH with the L gene from JPV-LW completely attenuates the resulting virus (rJPV-BH-LW-L) in BALB/c mice, demonstrating that these 3 amino acid differences play a critical role in pathogenicity[9].

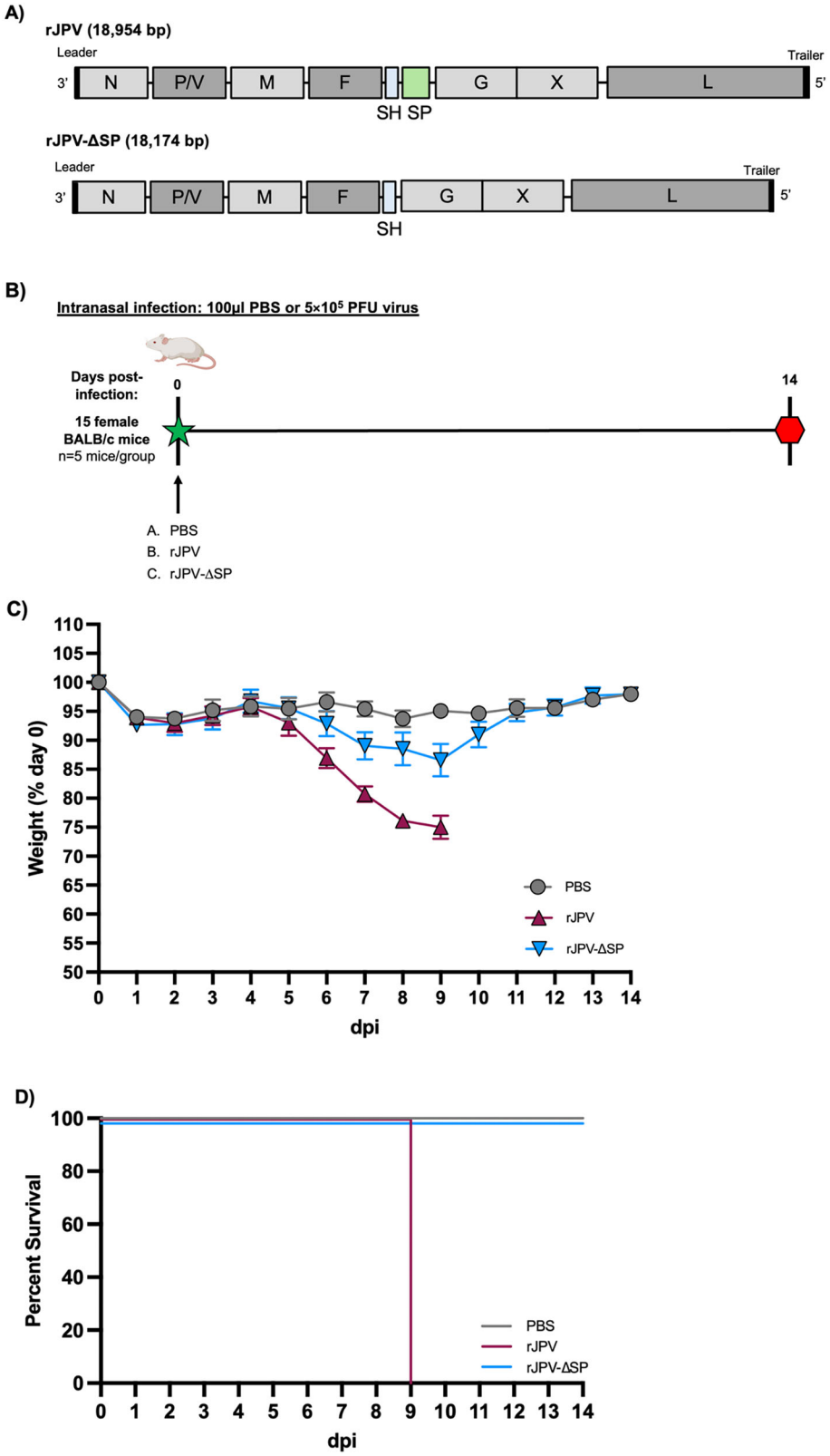

Fig. 1 | rJPV-ΔSP is partially attenuated in BALB/c mice. A Schematics of rJPV and rJPV-ΔSP showing the SP ORF deletion. **B** Female BALB/c mice were intranasally infected with 100 µl of PBS or 5×10^5 PFU of rJPV or rJPV-ΔSP (n = 5 mice per group). Mice were weighed daily for 14 dpi. **C** The mouse weights were monitored every day post-infection, and their percent body weight was compared to their pre-infection weight as percent of day 0. Horizontal bars represent the mean, and error bars represent the standard error of means. **D** Survival curve.

Using this knowledge, we generated a rJPV-Δ3 virus that possesses the L gene from the JPV-LW strain to promote attenuation in vivo (Fig. 5A). To examine if the LW-L gene altered viral growth, Vero cells were infected with either rJPV or JPV-Δ3-LW-L at an MOI of 0.1. The addition of the LW-L gene did not affect the ability of the virus to grow to higher titers as JPV-Δ3-LW-L had significantly higher viral titers than rJPV at 72, 96, and 120 hpi. (Fig. 5B).

rJPV-Δ3-LW-L is attenuated in vivo

To determine if rJPV-Δ3-LW-L was attenuated in vivo, mice were infected intranasally with 100 µl PBS or 1×10^6 PFU of rJPV or rJPV-Δ3-LW-L (n = 10/group) (Fig. 5C). All rJPV-infected mice had to be humanely euthanized by 4 dpi due to severe weight loss. In contrast, the rJPV-Δ3-LW-L-infected mice did not exhibit dramatic weight loss compared to the PBS group (Fig. 5D). All rJPV-Δ3-LW-L-infected mice survived and showed no

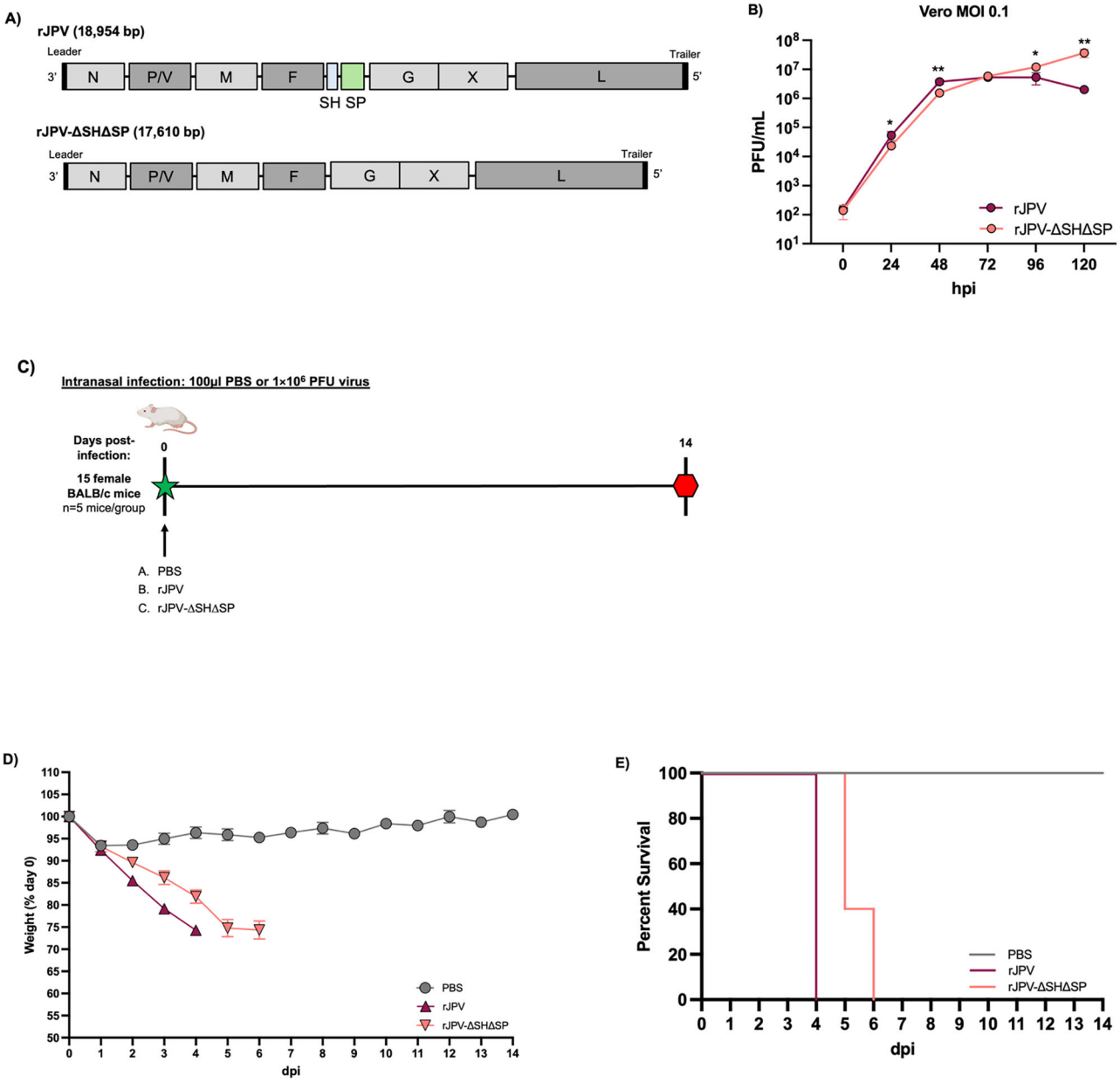

Fig. 2 | Generation and characterization of rJPV-ΔSHΔSP. A Schematics of rJPV and rJPV-ΔSHΔSP indicating the deletion of the SH and SP ORFs. **B** Comparison of rJPV and rJPV-ΔSHΔSP growth in vitro. Vero cells in a 6-well plate were infected, in triplicates, with rJPV or rJPV-ΔSHΔSP at an MOI of 0.1, and the medium was harvested every 24 h for 5 days. Plaque assays were performed on Vero cells to determine the virus titer. Error bars represent the standard error of the means, and statistical significance was calculated with t-tests. **C** Female BALB/c mice were intranasally infected with 100 µl of PBS or 1×10^6 PFU of rJPV or rJPV-ΔSHΔSP (n = 5 mice per group). **D** The mouse weights were monitored every day post-infection, and their percent body weight was compared to their pre-infection weight as percent of day 0. Horizontal bars represent the mean, and error bars represent the standard error of means. **E** Survival curve.

visible signs of illness throughout the study (Fig. 5E). Lungs were collected from 5 mice per group at 4 dpi to determine viral titers. rJPV-Δ3-LW-L-infected mice had significantly lower viral titers than the rJPV-infected mice. This demonstrates that rJPV-Δ3-LW-L is still detectable in the mouse lungs but does not replicate to as high a titer as rJPV (Fig. 5F).

Single intranasal immunization with rJPV-Δ3-LW-L protects mice against lethal JPV challenge

JPV is a paramyxovirus of the recently established *Jeilongvirus* genus, which is one of the most rapidly expanding genera in the *Paramyxoviridae* family[27]. While no jeilongviruses have emerged that are pathogenic in people or livestock, these viruses are being discovered at increasing rates in wildlife, mainly rodents and bats, which are known to harbor zoonotic viruses.

For example, a novel jeilongvirus was recently isolated from a wild rodent in Florida, USA and can replicate in various rodent, non-human primate, and human cell lines, demonstrating that this virus has potential to spillover[28]. It is imperative to have a prototype jeilongvirus vaccine in the event a species emerges that can infect humans and/or livestock and cause disease. Since rJPV-Δ3-LW-L was completely attenuated in mice, we wanted to assess its ability to induce protection against rJPV infection.

Mice were intranasally immunized with 1×10^6 PFU of rJPV-Δ3-LW-L (n = 5/group) (Fig. 6A). Mock-infected mice received an intranasal administration of 100 µl PBS. No significant weight differences were observed between the two groups following immunization (Fig. 6B). At 28 dpv, both groups were challenged with 1×10^6 PFU of rJPV. The PBS mice infected with rJPV experienced significant weight loss starting at 2 days post-challenge (dpc), while the rJPV-Δ3-LW-L-immunized mice

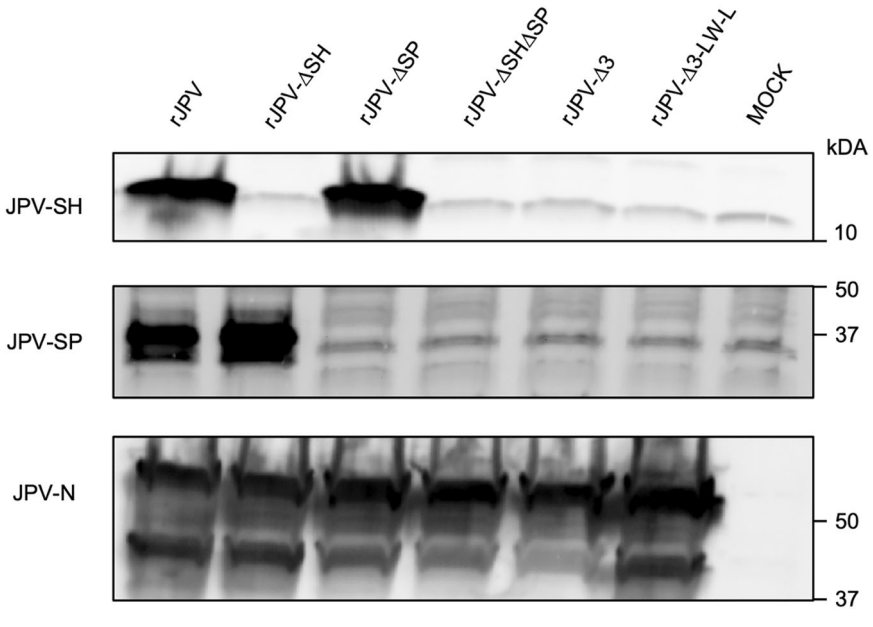

Fig. 3 | Protein expression of various rJPV knockout viruses. To confirm the deletion of SH and SP, Vero cells were infected with rJPV or the rJPV mutants (rJPV-ΔSH, rJPV-ΔSP, rJPV-ΔSHΔSP, rJPV-Δ3, rJPV-Δ3-LW-L) at an MOI of 0.1. Mock-infected cells served as the control. At 72 hpi, cell lysate was collected, mixed with loading buffer before being resolved by SDS-PAGE and immunoblotted using either an anti-JPV SH, anti-JPV-SP, or anti-JPV-N antibody.

remained at a healthy weight and showed no visible signs of disease (Fig. 6C). All PBS mice had succumbed to rJPV infection by 5 dpi, while the rJPV-Δ3-LW-L-immunized mice all survived (Fig. 6D). This demonstrates a single dose of the rJPV-Δ3-LW-L vector can induce complete protection from lethal jeilongvirus infection. At this point, we determined that the rJPV-Δ3-LW-L vector has superior growth in tissue culture, is attenuated in vivo, and can protect against JPV challenge. We then moved forward with using this vector to generate a vaccine candidate for NiV.

Generation and in vitro analysis of rJPV-Δ3-LW-L expressing NiV-F

In a plasmid containing the rJPV-Δ3-LW-L genome, the full-length fusion gene (NiV-F) from the NiV Malaysian strain was inserted in the place of JPV SH (rJPV-Δ3-NiV-F-LW-L) (Fig. 7A). After obtaining the rescued virus, the full-length genome sequence of purified rJPV-Δ3-NiV-F-LW-L was confirmed by Sanger sequencing. Expression of NiV-F in rJPV-Δ3-NiV-F-LW-L-infected Vero cells was confirmed via Western blot (Fig. 7B). To examine if insertion of NiV-F affects viral growth, Vero cells were infected with rJPV-Δ3-LW-L and rJPV-Δ3-NiV-F-LW-L at an MOI of 0.1. A similar growth pattern was observed for rJPV-Δ3-LW-L and rJPV-Δ3-NiV-F-LW-L, demonstrating that the insertion of NiV-F does not affect the ability of this virus to growth to a high titer in vitro (Fig. 7C).

Intranasal administration of rJPV-Δ3-NiV-F-LW-L induces NiV-F-specific antibodies in mice

To investigate the immune response generated by rJPV-Δ3-NiV-F-LW-L, we intranasally immunized mice with 100 µl of PBS or 1×10^6 PFU of rJPV-Δ3-LW-L or rJPV-Δ3-NiV-F-LW-L (Fig. 8A) and then boosted them 21 days later. The weight of animals was monitored for 14 dpi. No difference in the body weight was observed in mice inoculated with rJPV-Δ3-LW-L or rJPV-Δ3-NiV-F-LW-L compared to the PBS group, demonstrating that the vaccine is attenuated in mice (Fig. 8B). To measure humoral response induced by the recombinant JPV-NiV-F vaccine, mouse sera was collected two weeks post-prime and one week post-boost, and the anti-NiV-F antibody titer was quantified via ELISA. One dose of rJPV-Δ3-NiV-F-LW-L induced an anti-NiV-F humoral response, and following a boost, rJPV-Δ3-NiV-F-LW-L-vaccinated mice had a significantly higher antibody titer compared to post-prime (Fig. 8C, D).

rJPV-Δ3-NiV-F-LW-L-immunized hamsters are protected against lethal NiV-Malaysia challenge

Syrian hamsters are frequently used as a model for NiV infection, recapitulating neurological and respiratory disease progression observed in humans[29]. We evaluated the protective efficacy of rJPV-Δ3-NiV-F-LW-L vaccination in the Syrian hamster model of lethal NiV infection. Eighteen hamsters (9 M/9 F, n = 9/group) were intranasally immunized with 100 µl of PBS or 1×10^6 PFU of rJPV-Δ3-NiV-F-LW-L (Fig. 9A). At 21 dpv, all rJPV-Δ3-NiV-F-LW-L-vaccinated hamsters had developed anti-NiV-F IgG titers (Fig. 9B). To assess the functionality of vaccine-induced humoral responses, we tested the neutralization activity of the serum samples collected at 21 dpv against NiV-M. Six out of nine (66%) of the hamsters exhibited modest neutralization activity against NiV-M (Fig. 9C).

At 28 dpv, the hamsters were challenged intranasally with 1×10^6 $TCID_{50}$ of NiV-Malaysia (NiV-M). Body weight change, temperature, and clinical scores were measured for 28 dpc. While mock vaccinated control hamsters experienced significant weight loss post-challenge, the rJPV-Δ3-NiV-F-LW-L-immunized hamsters did not exhibit any weight loss (Fig. 9D). The body temperatures of the rJPV-Δ3-NiV-F-LW-L-vaccinated hamsters remained stable following challenge. However, at 4 dpc, one control hamster had a low body temperature consistent with terminal disease and met humane endpoint criteria due to severe clinical signs (Fig. 9D). Three other control hamsters had elevations in body temperature at the time of euthanasia associated with severe neurological manifestations, including seizures. All rJPV-Δ3-NiV-F-LW-L-vaccinated hamsters (9 of 9, 100%) survived challenge and exhibited no clinical signs of disease, whereas all control hamsters developed respiratory or neurological illness and 7 of 9 (78%) were humanely euthanized due to severity of disease (Fig. 9D).

Discussion

In this work, we developed a novel JPV vector with multiple alterations to its genome resulting in complete attenuation in a mouse model even at a high dose (1×10^6 PFU), protects against lethal JPV challenge, and can express a foreign antigen (NiV-F) and induce antigen-specific humoral responses in mice. Finally, we show that this novel vector expressing NiV-F induces complete protection against NiV-M challenge in hamsters. The use of rJPV as a vaccine vector was first introduced for influenza H5N1 by inserting HA in place of JPV SH[25]. rJPV-ΔSH-H5 protects mice from lethal HPAI H5N1 challenge and induces antigen-specific humoral and cellular immunity in rhesus macaques. A subsequent study generated a rJPV virus expressing HIV-env in place of JPV

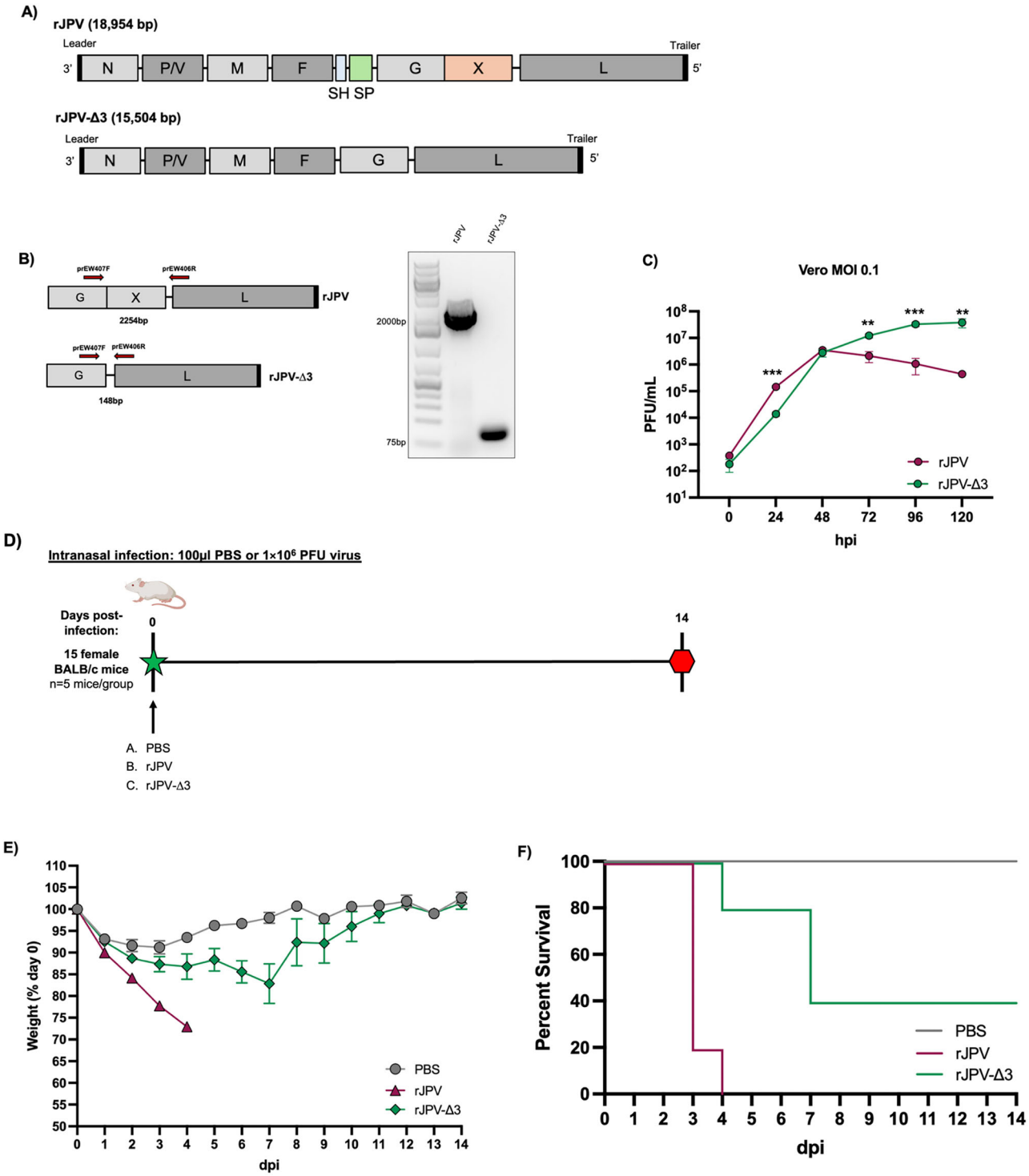

Fig. 4 | rJPV-Δ3 is recoverable but is still pathogenic in vivo. A Schematics of rJPV and rJPV-Δ3 indicating the deletion of the SH, SP, and X ORFs. **B** The ORF-X deletion was confirmed via reverse transcriptase PCR (RT-PCR) using primers that flank just outside of X. The expected sizes of the PCR products are 2254 bp (rJPV) and 148 bp (rJPV-Δ3). **C** Comparison of rJPV and rJPV-Δ3 growth in vitro. Vero cells in a 6-well plate were infected, in triplicates, with rJPV or rJPV-Δ3 at an MOI of 0.1, and the medium was harvested every 24 h for 5 days. Plaque assays were performed on Vero cells to determine the virus titer. Error bars represent the standard error of the means, and statistical significance was calculated with t-tests. **D** Female BALB/c mice were intranasally infected with 100 µl of PBS or 1×10^6 PFU of rJPV or rJPV-Δ3 (n = 5 mice per group). **E** The mouse weights were monitored every day post-infection, and their percent body weight was compared to their pre-infection weight as percent of day 0. Horizontal bars represent the mean, and error bars represent the standard error of means. **F** Survival curve.

SH[26]. The rJPV-ΔSH-env virus is still pathogenic in mice, indicating that the deletion of SH alone is not sufficient to attenuate the rJPV vector in mice. Even though rJPV-ΔSH-H5 was not pathogenic in non-human primates and there is no evidence of wild type JPV to be pathogenic in humans[25], we generated a series of rJPV mutants and assessed their pathogenicity in a mouse model to further reduce the potential of safety concern of JPV as a human vaccine vector.

We have previously shown that the JPV SP mediates cell-to-cell fusion[7], and that cleavage of SP is required for its syncytial-promoting activity[4]. While SP has been studied in vitro, its role in pathogenicity

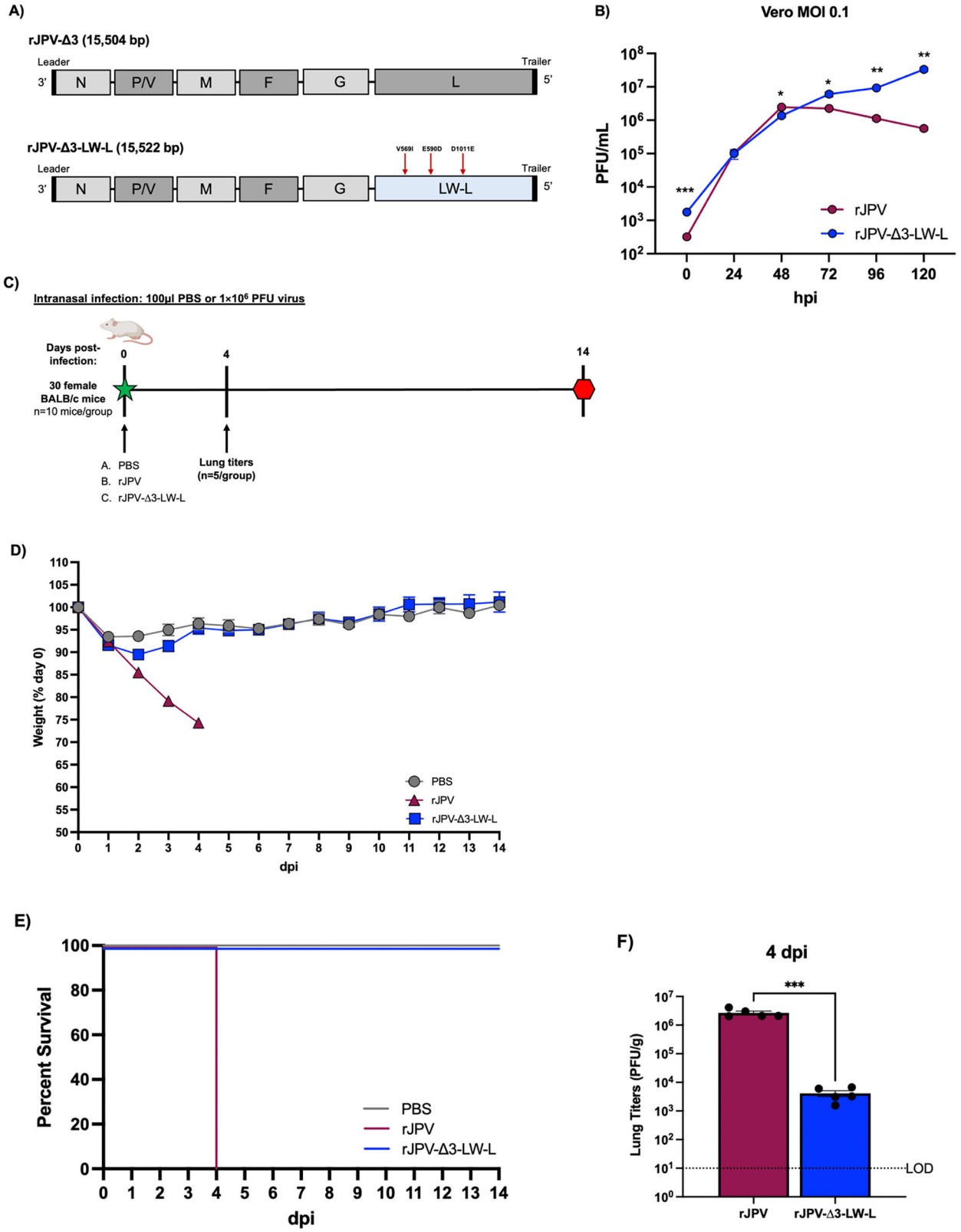

Fig. 5 | rJPV-Δ3-LW-L is attenuated in mice. A Schematics of rJPV-Δ3 and rJPV-Δ3-LW-L, with the amino acid residue differences in the L gene between the 2 viruses shown. **B** Comparison of rJPV and rJPV-Δ3-LW-L growth in vitro. Vero cells in a 6-well plate were infected in triplicates with either rJPV or rJPV-Δ3-LW-L at an MOI of 0.1, and the medium was harvested every 24 hours for 5 days. Plaque assays were performed on Vero cells to determine the virus titer. Error bars represent the standard error of the means, and statistical significance was calculated with t-tests. **C** Female BALB/c mice were intranasally infected with 100 µl of PBS or 1×10^6 PFU of rJPV or rJPV-Δ3-LW-L (n = 10 mice per group). **D** The mouse weights were monitored every day post-infection, and their percent body weight was compared to their pre-infection weight as percent of day 0. Horizontal bars represent the mean, and error bars represent the standard error of means. **E** Survival curve. **F** Mouse lungs were collected at 4 dpi (n = 5/group). Virus titers were determined by plaque assay on Vero cells.

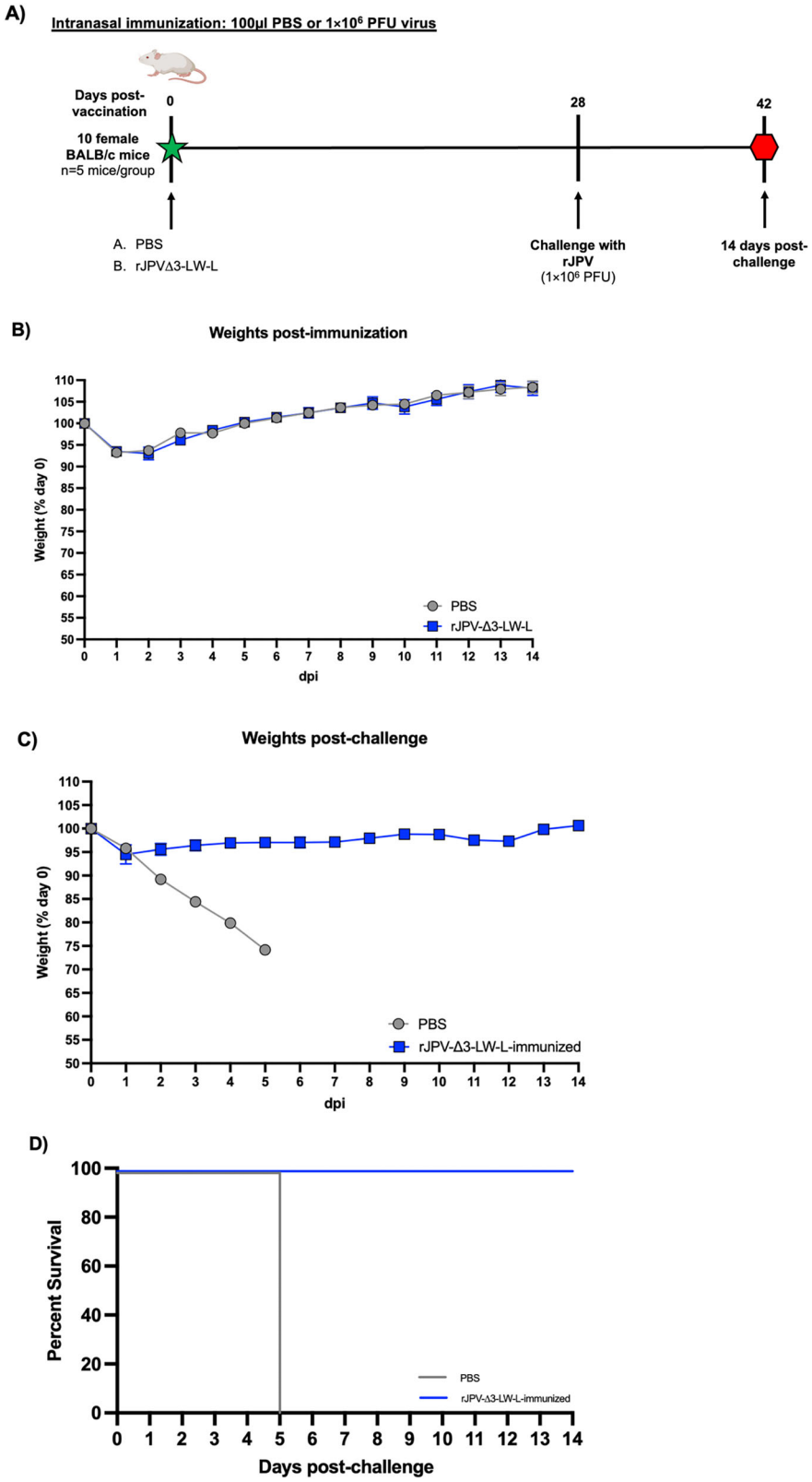

Fig. 6 | Single intranasal immunization with rJPV-Δ3-LW-L protects against lethal JPV challenge. **A** Female BALB/c mice were intranasally immunized with 100 µl of PBS or 1×10^6 PFU of rJPV-Δ3-LW-L (n = 5 mice per group). At 28 dpv, mice were challenged with 1×10^6 PFU of rJPV. **B** Mouse weights post-immunization. The mouse weights were monitored every day post-immunization, and their percent body weight was compared to their pre-infection weight as percent of day 0. Horizontal bars represent the mean, and error bars represent the standard error of means. **C** Mouse weights post-JPV challenge. **D** Survival curve post-JPV challenge.

remained unknown. Our data indicate SP plays a role in pathogenesis (Fig. 1C, D). rJPV-ΔSP was attenuated in mice. However, rJPV-ΔSP still caused about 12% weight loss, indicating rJPV-ΔSP is still pathogenic in animal.

Because the deletion of SH and SP separately results in partial attenuation, we generated a rJPV that lacks expression of both these proteins (Fig. 2A). Interestingly, rJPV-ΔSHΔSP was pathogenic and caused mortality in animals (Fig. 2D, E), while rJPV-ΔSP only caused weight loss. While the function of X is unknown, we generated the rJPV-Δ3 virus that had the ORFs of SH, SP, and X deleted (Fig. 4A). rJPV-Δ3 had reduced pathogenicity compared to rJPV-ΔSHΔSP but still caused disease and 60% of the infected mice had to be humanely euthanized due to severe weight loss (Fig. 4E, F). However, these results indicate that the X ORF may be contributing

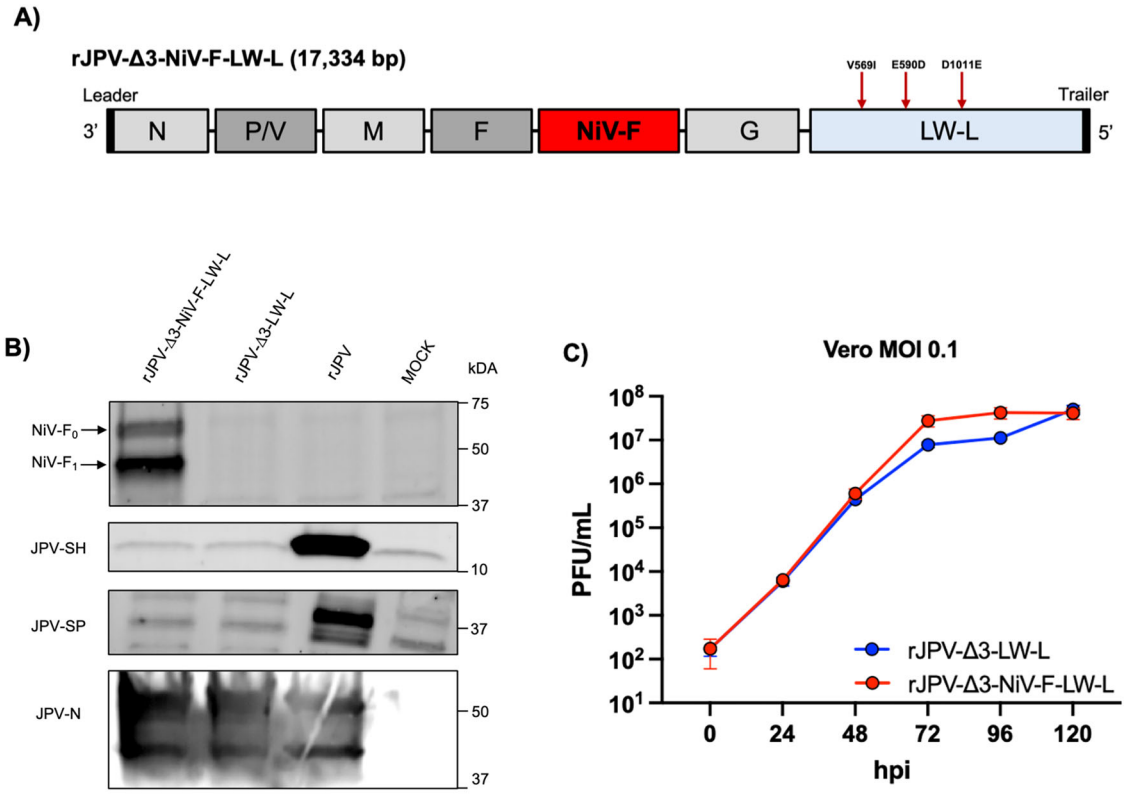

Fig. 7 | Generation and in vitro characterization of rJPV-Δ3-LW-L expressing NiV-F. A Schematics of rJPV-Δ3-NiV-F-LW-L, indicating the location where the ORF of SH was replaced with NiV-F. The SP and X ORFs are also deleted, along with several mutations in the L gene from the rJPV-LW strain to attenuate the virus in vivo. **B** Confirm rJPV-Δ3-NiV-F-LW-L expression of NiV-F via Western blot. Vero cells were infected with rJPV, rJPV-Δ3-LW-L, or rJPV-Δ3-NiV-F-LW-L at an MOI of 0.1. At 72 hpi, cell lysate was collected, mixed with loading buffer before being resolved by SDS-PAGE and immunoblotted using either an anti-JPV SH, anti-JPV- SP, anti-JPV-N, or anti-NiV-F antibody. **C** Comparison of JPV-Δ3-LW-L and JPV-Δ3-NiV-F-LW-L growth in vitro. To determine if the NiV-F gene affects viral growth, Vero cells in a 6-well plate will be infected, in triplicates, with either virus at an MOI of 0.1. The medium was collected every 24 h for 5 days. The titers were determined by plaque assay on Vero cells. Error bars represent the standard error of the means, and statistical significance was calculated with t-tests.

to pathogenicity as its deletion partially attenuated the virus. Future studies are needed to examine the role of X in virulence in vivo.

We further attenuated rJPV-Δ3 by replacing the 3 amino acid residues that are different from the attenuated rJPV-LW strain (Fig. 5A). It is thought that the non-pathogenic rJPV-LW is a laboratory adapted strain of rJPV-BH, which causes severe disease in mice. Replacement of the L gene in rJPV-BH with the L gene from the LW strain results in complete viral attenuation in mice[9]. rJPV-Δ3 with the L gene from the JPV-LW strain, termed rJPV-Δ3-LW-L, grew significantly better than rJPV in Vero cells (Fig. 5B). BALB/c mice were intranasally infected with 1×10^6 PFU of either rJPV or rJPV-Δ3-LW-L (Fig. 5C). All rJPV-infected mice had to be humanely euthanized by 4 dpi due to severe weight loss, while the rJPV-Δ3-LW-L all survived and did not experience any significant weight loss compared to the PBS mice (Fig. 5D, E), demonstrating that the addition of the LW-L gene completely attenuates the rJPV-Δ3 vector.

The *Jeilongvirus* genus was proposed in 2016. Novel jeilongviruses are being discovered worldwide in wildlife populations at increasing rates, mainly in bats and rodents[27]. For example, a novel jeilongvirus was recently isolated from a wild rodent from Gainesville, Florida, USA[28]. Jeilongviruses have high zoonotic potential as these mammalian hosts are natural reservoirs of many zoonotic paramyxoviruses that significantly impact public health, such as NiV and Hendra virus (HeV)[30]. It is imperative to develop a jeilongvirus prototype vaccine in the event one of these viruses spills over into humans or livestock. Mice were intranasally immunized with 100 µL PBS or 1×10^6 PFU of rJPV-Δ3-LW-L, and at 28 dpv, challenged with a lethal dose of rJPV (Fig. 6A). All PBS mice succumbed to infection by 5 dpc, while all rJPV-Δ3-LW-L-immunized mice survived and did not lose weight or display signs of disease (Fig. 6C, D). These results demonstrate that the strategy employed to attenuate rJPV-Δ3-LW-L can potentially be applied to develop a vaccine for any emerging jeilongviruses.

We examined the immunogenicity in rJPV-Δ3-NiV-F-LW-L in BALB/c mice (Fig. 8A). Mice intranasally immunized with 1×10^6 PFU of rJPV-Δ3-NiV-F-LW-L exhibited no signs of illness or significant weight loss compared to the PBS mice (Fig. 8B). Intranasal immunization with rJPV-Δ3-NiV-F-LW-L induced NiV-F-specific antibodies in the mice (Fig. 8C). For viral-vectored vaccines, pre-existing immunity can negatively impact vaccine efficacy[31]. We have previously reported that rJPV vaccination can overcome pre-existing immunity in rhesus macaques, as one immunization of rJPV-ΔSH-H5 induced anti-H5 IgG antibodies in the animals and a boost 28 days later resulted in an approximate 10-fold increase in antibody titer[25]. However, in comparing anti-HIV-env antibody responses in mice immunized with 2 doses of rJPV-ΔSH-env, there was no significant increase in mean IgG titer post-boost[26]. Because JPV is a rodent virus, it may replicate better in the mice than in macaques. There may have been anti-JPV antibodies of high enough titer to negatively affect the second dose of rJPV-ΔSH-env in the mice but not in the macaques[26]. In this experiment, mice were primed with 1×10^6 PFU of rJPV-Δ3-NiV-F-LW-L and boosted with the same dose 3 weeks later. Blood was taken for ELISAs at 14 days post-prime and 7 days post-boost. Interestingly, anti-NiV-F IgG titers were significantly higher post-boost when compared to the post-prime titers (Fig. 8C).

Finally, we assessed the immunogenicity and protective efficacy of rJPV-Δ3-NiV-F-LW-L in Syrian hamsters (Fig. 9A). All hamsters vaccinated with rJPV-Δ3-NiV-F-LW-L developed anti-NiV-F IgG titers at 21 dpv (Fig. 9B). At 28 dpv, the hamsters were challenged with NiV-M. The control hamsters began losing weight following challenge, while the body

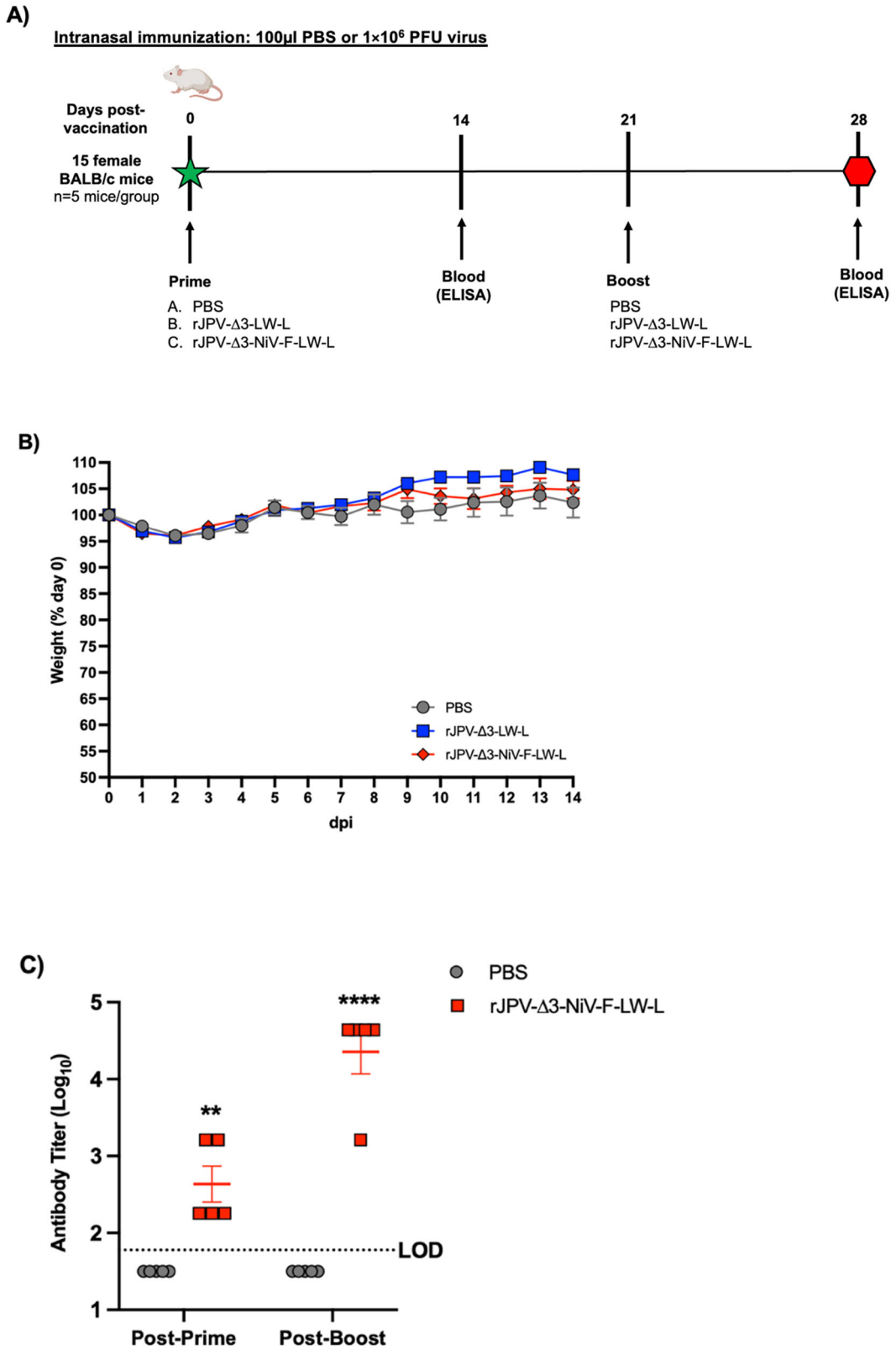

Fig. 8 | Immunization of BALB/c mice with rJPV-Δ3-NiV-F-LW-L. A Mice were intranasally primed with 100 µl of PBS, rJPV-Δ3-LW-L, or rJPV-Δ3-NiV-F-LW-L at a dose of 1×10^6 PFU (n = 5 per group). At 21 dpi, the mice were boosted with the same viral dose. **B** Mice were monitored daily for 14 days after being primed, and weight loss was graphed as the average percentage of their original weight (on the day of infection). **C** Blood was collected at 14 days post-prime and 7 days post-boost, and anti-NiV-F IgG antibody titers were quantified via ELISA. The limit of detection (LOD) is indicated by the dotted line. Error bars represent the standard error of the means, and statistical significance was calculated with t-tests.

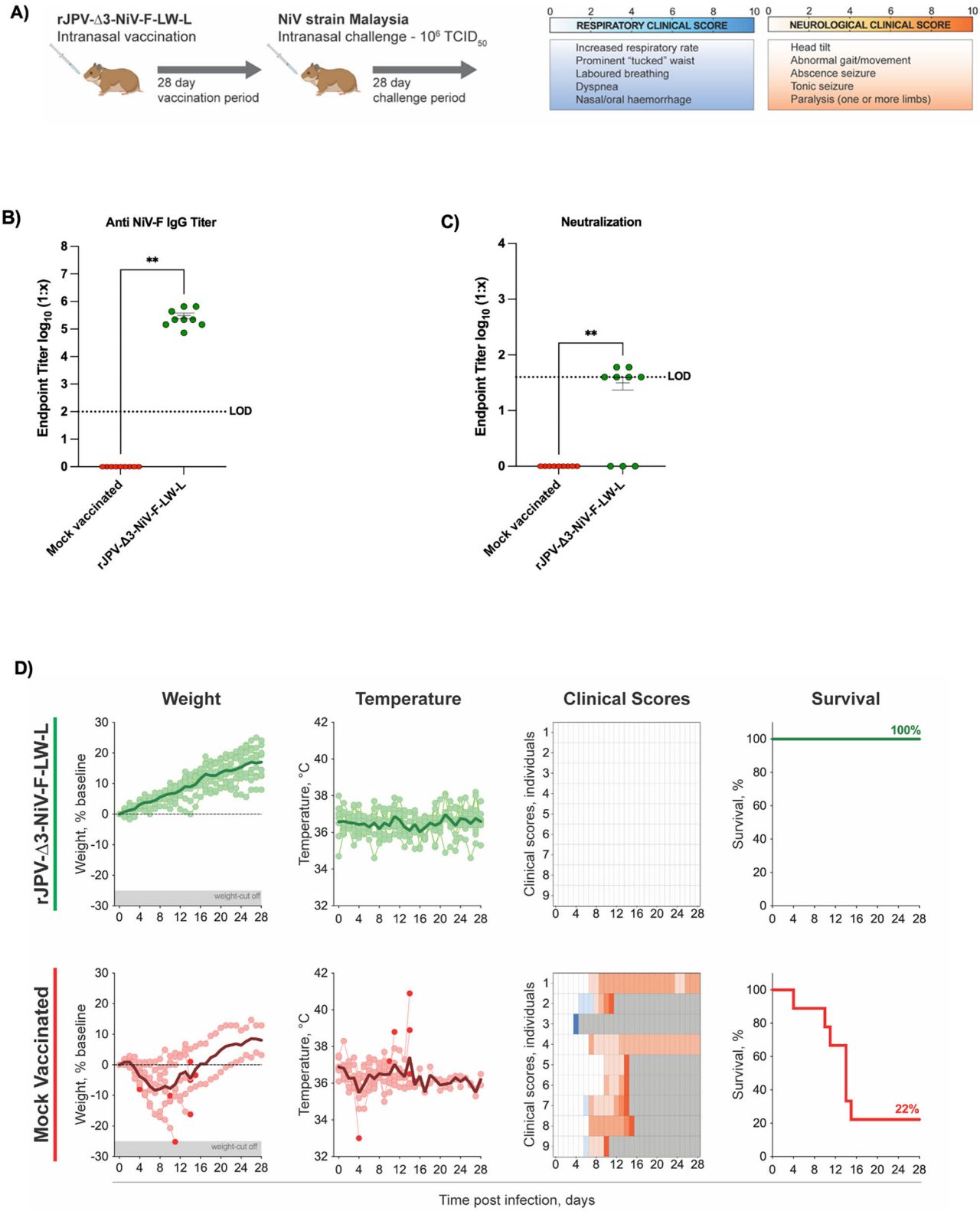

Fig. 9 | Intranasal NiV strain Malaysia challenge in rJPV-Δ3-NiV-F-LW-L-vaccinated hamsters. A Syrian hamsters (n = 9 per group) were intranasally immunized with 100 µl of PBS or 1×10^6 PFU of rJPV-Δ3-NiV-F-LW-L, then at 28 dpv challenged intranasally with 1×10^6 $TCID_{50}$ of NiV strain Malaysia and monitored for 28 dpc. **B** Antibody titer and (**C**) neutralization activity of serum samples collected at 21 dpv. The limit of detection (LOD) is indicated by the dotted line. Error bars represent the standard error of the means, and statistical significance was calculated with t-tests. **D** Clinical data for animals vaccinated with rJPV-Δ3-NiV-F-LW-L (green) or mock vaccinated with PBS alone (red), with plots representing (left to right): percent weight change from baseline (taken at 0 dpi); body temperature; daily clinical scores; and overall survival. For weight and temperature, each circle represents an individual animal; bold circles indicate an animal that succumbed to infection on that day, and the solid line denotes the daily mean. For clinical scores, animals were evaluated daily on a 0 to 10 scale, with representative clinical signs and scale bar shown in the top right of figure. Severity is indicated by increasing intensity of blue (respiratory signs) or red (neurological signs). Animals scoring ≥10 were humanely euthanized, and any animal that succumbed to disease prior to euthanasia was allocated a score of 10. Grey boxes indicate the end of monitoring and scoring due to euthanasia or death.

weights of the vaccinated hamsters showed no significant body weight decline (Fig. 9D). The body temperatures of the vaccinated hamsters remained stable after challenge while temperature fluctuations were detected in multiple control hamsters (Fig. 9D). All the rJPV-Δ3-NiV-F-LW-L-vaccinated hamsters survived the challenge with no clinical disease detected, whereas only 22% of the control hamsters survived and all of them showed clinical signs of disease (Fig. 9D). This study demonstrates that rJPV-Δ3-NiV-F-LW-L offers complete protection against lethal NiV challenge in an animal model.

An in vitro assay measuring neutralizing antibodies against NiV-M in serum samples collected at 21 dpv was performed. Low levels of neutralizing antibodies against NiV-M were detected in 6 out of 9 of the rJPV-Δ3-NiV-F-LW-L-vaccinated hamsters, although all 9 survived challenge and never showed signs of disease (Fig. 9C). The lack of robust neutralizing titers suggests that other antibody functions, such as complement deposition and phagocytosis, may have played a role in protecting the vaccinated hamsters from disease.

Additional assays further defining the humoral response functionality profile induced by our vaccine platform will need to be performed. Cell-mediated immunity may have also contributed to the protective efficacy induced by the rJPV-Δ3-NiV-F-LW-L vaccination and will need to be assessed in follow-up vaccine studies. Future experiments are also needed to examine the safety and efficacy of our novel JPV vector in other species and determine its tissue tropism in vivo. Overall, this study supports the use of rJPV-Δ3-LW-L as both a jeilongvirus vaccine and for viral-vectored vaccine development.

Methods

Cells

Vero cells were maintained in Dulbecco's modified Eagle media (DMEM) supplemented with 5% fetal bovine serum (FBS) plus 100 IU/mL penicillin and 100ug/mL streptomycin (1% P/S; Mediatech Inc, Manassas, VA, USA). Cells were incubated at 37 °C, 5% CO_2. Infections were done in DMEM + 2% FBS + 1% P/S.

Plasmids and virus rescue

The construction of a recombinant JPV plasmid[9] and a recombinant JPV-ΔSH-GFP have been previously described[6]. For this study, we assessed 4 different rJPV mutants for use as a vaccine vector: rJPV-ΔSP, rJPV-ΔSHΔSP, rJPV-Δ3, and rJPV-Δ3-LW-L. The pJPV-ΔSP was generated previously by deleting the SP ORF[7]. To generate pJPV-ΔSHΔSP, the ORFs for the SH gene and the SP gene were deleted. The pJPV-Δ3 had the SH, SP, and X ORFs deleted. The JPV-BH L gene was then replaced with the L gene from the JPV-LW strain to generate the pJPV-Δ3-LW-L plasmid. To create an intranasal NiV vaccine candidate, the NiV-Malaysia fusion gene (NiV-F) was cloned into the place of the SH ORF (pJPV-Δ3-NiV-F-LW-L). Primer sequences are available upon request. To generate these viruses, HEK293T cells, 60% confluent in a 6 cm dish, were transfected with Lipofectamine® 3000 (Invitrogen, Waltham, MA), 1 μg full-length JPV genome plasmid and the helper plasmids 0.1 μg pJPV-N, 0.05 μg pJPV-P, 3.75 μg pJPV-L, and 1 μg pT7-polymerase. The plasmid containing the full-length JPV genome is under control of a T7 RNAP promoter[32]. The T7 polymerase transcribes the JPV cDNA into positive-sense antigenome. The helper plasmids provide the viral N, P, and L proteins, which replicate and transcribe the antigenome into the negative-sense viral RNA genome. The helper plasmids are under the control of a CAG promoter.

After 24 hours, the transfection medium was removed from the HEK293T cells and the cells were trypsinized and resuspended in 2 ml of 5% FBS, 1% P/S DMEM. These cells were then co-cultured with 4 ml of resuspended Vero cells into a 10-cm plate. The co-culture was brought to 10 ml total with the addition of an 4 ml of 5% FBS, 1% P/S DMEM to the plate. The media was harvested between days 7–14 after co-culture. Plaque assays on Vero cells were used to isolate single clones of recombinant viruses. RNA from propagation media was isolated with the RNeasy minikit (Qiagen, Valencia, CA). Reverse transcription-polymerase chain reaction (RT-PCR) was performed to generate overlapping sections of the genome, and multiple primers were used to sequence each section. Sequencing results were analyzed in Sequencher (Gene Codes Corporation, Ann Arbor, MI).

JPV propagation

The recombinant JPV viruses were propagated in Vero cells. The cells were infected at an MOI of 0.1 in DMEM supplemented with 1% bovine serum albumin (BSA) and 1% P/S. After 1 hour, the infection media was replaced with DMEM plus 2% FBS and 1% P/S. After 5 to 7 days of incubation at 37°C with 5% CO_2, the media was collected and centrifuged at 1000 rpm for 5 mins to pellet cell debris. The supernatant was mixed with 0.1 volume of 10X sucrose-phosphate-glutamate (SPG) buffer, aliquoted, flash-frozen in liquid nitrogen, and stored at −80 °C. The rJPV virus stocks were titrated via plaque assay in Vero cells.

Detection of viral protein expression

To detect expression of various JPV proteins and NiV-F, Western blots were performed. Vero cells were infected at an MOI of 0.1 with rJPV, rJPV-ΔSH, rJPV-ΔSP, rJPV-ΔSHΔSP, rJPV-Δ3, rJPV-Δ3-LW-L, or rJPV-Δ3-NiV-F-LW-L. Mock-infected cells were used as a control. At 72 hpi, the cells were lysed in 2X Laemmli + 2-mercaptoethanol and heated at 95 °C for five minutes. The lysates were run on an SDS-PAGE gel, transferred to a Hamersham Hybond-LFP membrane (GE), and incubated overnight at 4 °C with the primary antibody diluted in PBS + 3% nonfat milk. The in-house primary JPV antibodies used were anti-JPV-SH (diluted 1:200), anti-JPV-SP (diluted 1:500), and anti-JPV-N (diluted 1:1000). The NiV-F primary antibody was used at a 1:1000 dilution (Absolute Antibody; Catalog No. Ab02855-3.0). The following day, the membranes were washed with PBS + 0.1% Tween-20 (PBST) and incubated with anti-mouse or anti-rabbit Cy3 (Abcam) at 1:1000 in PBS + 2% nonfat milk for 1 h. The membranes were washed with PBST and imaged with a BioRad ChemiDoc MP Imaging System.

Growth kinetics

Vero cells in 6-well plates were infected with rJPV, rJPV-ΔSHΔSP, rJPV-Δ3, rJPV-Δ3-LW-L, or rJPV-Δ3-NiV-F-LW-L at an MOI of 0.1. The cells were then washed with PBS and maintained in 2% FBS, 1% P/S DMEM. The medium was collected at 0, 24, 48, 72, and 96 hpi. The titers were determined by a plaque assay on Vero cells.

Mouse studies

Six- to eight-week-old female BALB/c (Envigo) were used in this study. Mouse infections were done in enhanced biosafety level 2 facilities in HEPA-filter isolators. Mice were anesthetized by intraperitoneal (IP) injection of 250 μl 2,2,2-tribromoethanol in tert-amyl alcohol (Avertin). For the first pathogenicity study examining the SP deletion, the anesthetized mice were intranasally inoculated with 100 μl of phosphate-buffered saline (PBS) or 5×10^5 PFU of rJPV or rJPV-ΔSP (n = 5/group). For all subsequent pathogenicity studies, the mice were intranasally inoculated with 100 μl of PBS or 1×10^6 PFU of rJPV or rJPV mutant virus (rJPV-ΔSHΔSP (n = 5/group), rJPV-Δ3 (n = 5/group), or rJPV-Δ3-LW-L (n = 10/group)). In the rJPV-Δ3-LW-L pathogenicity study, lungs were collected from 5 mice per group at 4 dpi to quantify viral lung titers via plaque assays using Vero cells. For the challenge study (n = 5/group), PBS mice and rJPV-Δ3-LW-L-immunized mice were intranasally infected with 1×10^6 PFU of rJPV at 28 dpv. For the NiV vaccine study (n = 5/group), mice were primed with 100 μl of PBS or 1×10^6 PFU of rJPV-Δ3-LW-L or rJPV-Δ3-NiV-F-LW-L. Blood was collected via cheek bleeds at 14 dpv. At 21 days post-prime, the mice were boosted with the same viral dose. At 7 days post-boost, the mice were euthanized, and serum was collected via cardiothoracic bleeds. For all studies, the mice were weighed daily for the first 14 dpi. Any mice that dropped below 80% of starting body weight for more than 24 h were humanely euthanized, as specified in our AUP. Mice were euthanized by an anesthetic overdose (500 μl Avertin IP injection) followed by cervical dislocation to ensure death. This method is consistent

with the recommendations of the American Veterinary Medical Association (AVMA) Guidelines.

In vivo Nipah virus challenge studies

Groups of outbred Syrian hamsters (n = 9 per group; 4–5 females and 4–5 males, 3–5 weeks of age; HsdHan®:AURA, Envigo; Cat. No. 8902 M and 8902 F) were vaccinated intranasally with 1×10^6 PFU of rJPV-Δ3-NiV-F-LW-L or mock-vaccinated (PBS alone) 28 days prior to virus challenge. The hamsters were anesthetized for vaccination with 4% isoflurane. For blood collection post-vaccination, the hamsters were anesthetized with a mixture of ketamine (130–150 mg/kg) and xylazine (4–6 mg/kg). Blood (up to 0.5 ml) was collected via gingival vein. At 21 dpv, blood was collected from the hamster gingival vein to measure serum NiV-F-specific IgG responses and neutralizing antibody titers against NiV.

All hamsters were challenged intranasally with NiV strain Malaysia (target dose: 1×10^6 $TCID_{50}$; actual dose: 8.02×10^5 $TCID_{50}$) on day 0. NiV strain Malaysia (GenBank: AF212302; CDC Virharv #813744) originated from a 1999 human clinical isolate (cerebrum) and was passaged once on Vero E6 cells for virus isolation from a cerebrum sample, then further amplified on Vero cells.

Hamsters were housed in a climate-controlled laboratory with a 12 h day/night cycle; provided commercially available rodent chow and water ad libitum; and group-housed on corn cob bedding (Bed-o'Cobs ¼", Anderson Lab Bedding) with crinkle paper (Enviro-Dry), soft/ultra absorbent bedding (Carefresh) and cotton nestlets in an isolator-caging system (Tecniplast GR900 cages, West Chester, PA, USA) with a HEPA-filtered inlet and exhaust air supply. Microchip transponders (BMDS IPTT-300) were placed subcutaneously in the interscapular region for identification and body temperature assessment. Baseline weights were taken before challenge (0 dpc), and hamsters were assessed daily up to 28 dpc to record weight change, body temperature and score clinical signs. Animals were scored by the following criteria: quiet dull responsive, hunched back/ruffled coat, hypoactivity, mild neurological signs—each 2 points; abnormal breathing (e.g., increased respiratory rate, dyspnea), hypothermia (<34 °C), moderate neurological signs—each 5 points; paralysis, frank hemorrhage, moribund, weight loss >25% of baseline, severe neurological signs—each 10 points. Neurological signs were classified as: mild - abnormal gait or movement, mild (~0–30° from vertical) or sporadic head tilt; moderate - tremors, ataxia, circling, absence seizures, moderate (~>30–90° from vertical) and persistent head tilt while retaining ability to walk, eat, and drink; severe – limb paralysis, tonic clonal seizure, inability to right, severe (>90° from vertical) head tilt. Hamsters were euthanized with isoflurane vapor when they met euthanasia criteria (score ≥10) or at the completion of the study (28 dpc).

The vaccination procedures were conducted in biosafety level 2 facilities at the University of Georgia Biological Sciences Animal Facility (Athens, Georgia, USA). Animal experiments were performed in accordance with the national guidelines provided by "The Guide for Care and Use of Laboratory Animals" and the University of Georgia Institutional Animal Care and Use Committee (IACUC). The IACUC of the University of Georgia approved all animal experiments.

All NiV infections were performed in biosafety level 4 facilities at the Centers for Disease Control and Prevention (Atlanta, GA, USA). All animal procedures were approved by the CDC IACUC (#3419SPEMULC) and conducted in accordance with the Guide for the Care and Use of Laboratory Animals. The CDC is fully accredited by the AAALAC-International.

Enzyme-linked immunosorbent assay (ELISA)

To quantify the anti-NiV-F humoral response post-prime and post-boost, mouse serum was analyzed via ELISA. Immulon® 2HB 96-well microtiter plates were coated with 100 µl NiV-F protein (Creative Diagnostics; DAG-WT633) at 1 µg/ml. The serum was serial diluted three-fold starting at a 1:60 dilution and incubated on the plates for 2 h. Horseradish peroxidase-labelled goat anti-mouse IgG secondary antibody (Southern Biotech, Birmingham, Alabama) was diluted 1:2000 and incubated on the wells for 1 h. The plates were developed with KPL SureBlue Reserve TMB Microwell Peroxidase Substrate (SeraCare Life Sciences, Inc., Milford, Massachusetts), and OD_{450} values were detected with a BioTek Epoch Microplate Spectrophotometer (BioTek, Winooski, Vermont). Antibody titers were calculated as $\log_2$ or $\log_{10}$ of the highest serum dilution at which the OD_{450} was greater than two standard deviations above the mean OD_{450} of naïve serum.

To quantify the anti-NiV-F humoral response in the hamsters, Immulon 2HB plates were coated with 100 µl of 1 µg/mL NiV-F protein (DAG-WT633, Creative Diagnostics) in PBS and incubated overnight at 4 °C. Wells were washed 3× with 300ul PBS-T (0.1% Tween-20 in PBS) and blocked (5% w/V non-fat dry milk in PBST) for 1 h at RT. Following blocking, the buffer was decanted, and 100 µl of hamster plasma prepared in blocking buffer with 3-fold serial dilutions (ranging from 1:100 to 1:5,904,900) was added to the wells in duplicate. After 1 hour incubation at RT, wells were washed 3×, anti-hamster IgG HRP (1:10000, Invitrogen, #PA1-29626) was added to the wells (100 µL), and plates were incubated for 1 h at RT. Following incubation, wells were washed 3×, and 100 µl TMB Ultra ELISA substrate (Thermo Fisher) was added and incubated for 10 min at RT. The reaction was stopped by adding ELISA stop solution (Thermo Fisher), and optical density was read at 450 nm on BioTek Epoch microplate reader. The signal from the negative control wells without plasma samples was subtracted from the reads, and cut-off value was determined for each plate based on the average absorbance value of the wells with naïve hamster plasma plus 3 standard deviations. The highest dilutions with a signal above the determined cut-off value were assigned as the endpoint titers.

Neutralization assay

Serum samples were heat-inactivated for 30 minutes at 56 °C. Each serum sample was tested in duplicate for neutralizing antibodies against NiV-M. The sera samples were serially diluted two-fold in DMEM to allow testing in a dilution range of 1:40–1:5120. Also evaluated were controls diluted in an equivalent dilution series consisting of: negative inhibition control, normal uninfected mouse sera; and positive assay control, rabbit polyclonal sera produced against soluble Hendra virus F protein (Genscript). After dilution, all samples were incubated for 1 h at 37 °C with 200 $TCID_{50}$ of NiV-M before being added Vero cells in 96-well plates and incubated at 37 °C for 7 days. The cell monolayers were then fixed with formalin and stained with crystal violet to score cell cytopathic effect. Samples with one duplicate positive at 1:40 and one negative were recorded as below limit of detection (BLD).

Statistical analysis

Statistical significance was calculated with t-tests (****, $P < 0.0001$; ***, $P < 0.001$; **, $P < 0.01$; * $P \leq 0.05$) using Graphpad Prism software 7.

Data availability

Data is provided in the manuscript or supplementary files. The data used or analyzed for this study are available from the corresponding author on request.

Received: 21 March 2025; Accepted: 15 December 2025;
Published online: 06 January 2026

References

1. Jun, M. H., Karabatsos, N. & Johnson, R. H. A new mouse paramyxovirus (J virus). *Aust. J. Exp. Biol. Med. Sci.* **55**, 645–647 (1977).
2. Jack, P. J., Boyle, D. B., Eaton, B. T. & Wang, L. F. The complete genome sequence of J virus reveals a unique genome structure in the family paramyxoviridae. *J. Virol.* **79**, 10690–10700 (2005).
3. Vanmechelen, B. et al. Discovery and genome characterization of three new Jeilongviruses, a lineage of paramyxoviruses characterized by their unique membrane proteins. *BMC Genomics* **19**, 617 (2018).
4. An, D. et al. Cleavage of the syncytial protein of J paramyxovirus is required for its ability to promote cell-cell fusion. *Proc. Natl. Acad. Sci. USA* **121**, e2403389121 (2024).

5. Li, Z. et al. Function of the small hydrophobic protein of J paramyxovirus. *J. Virol.* **85**, 32–42 (2011).
6. Abraham, M. et al. Role of small hydrophobic protein of J paramyxovirus in virulence. *J. Virol.* **92**, e00653-18 (2018).
7. Li, Z. et al. Type II integral membrane protein, TM of J paramyxovirus promotes cell-to-cell fusion. *Proc. Natl. Acad. Sci. USA* **112**, 12504–12509 (2015).
8. Jack, P. J. M. et al. Expression of novel genes encoded by the paramyxovirus J virus. *J. Gen. Virol.* **89**, 1434–1441 (2008).
9. Li, Z. et al. The L gene of J paramyxovirus plays a critical role in viral pathogenesis. *J. Virol.* **87**, 12990–12998 (2013).
10. Epstein, J. H. et al. Nipah virus dynamics in bats and implications for spillover to humans. *Proc. Natl. Acad. Sci. USA* **117**, 29190–29201 (2020).
11. Clayton, B. A., Wang, L. F. & Marsh, G. A. Henipaviruses: an updated review focusing on the pteropid reservoir and features of transmission. *Zoonoses Public Health* **60**, 69–83 (2013).
12. Clayton, B. A. Nipah virus: transmission of a zoonotic paramyxovirus. *Curr. Opin. Virol.* **22**, 97–104 (2017).
13. Loomis, R. J. et al. Structure-based design of Nipah virus vaccines: a generalizable approach to paramyxovirus immunogen Development. *Front. Immunol.* **11**, 842 (2020).
14. Luby, S. P. The pandemic potential of Nipah virus. *Antiviral. Res.* **100**, 38–43 (2013).
15. Aditi & Shariff, M. Nipah virus infection: a review. *Epidemiol. Infect*. **147**, e95 (2019).
16. Loomis, R. J. et al. Chimeric cusion (F) and attachment (G) glycoprotein antigen delivery by mRNA as a candidate Nipah vaccine. *Front. Immunol.* **12**, 772864 (2021).
17. Walpita, P. et al. A VLP-based vaccine provides complete protection against Nipah virus challenge following multiple-dose or single-dose vaccination schedules in a hamster model. *npj Vaccines* **2**, 21 (2017).
18. Guillaume, V. et al. Nipah virus: vaccination and passive protection studies in a hamster model. *J. Virol.* **78**, 834–840 (2004).
19. Weingartl, H. M. et al. Recombinant Nipah virus vaccines protect pigs against challenge. *J. Virol.* **80**, 7929–7938 (2006).
20. van Doremalen, N. et al. A single-dose ChAdOx1-vectored vaccine provides complete protection against Nipah Bangladesh and Malaysia in Syrian golden hamsters. *PLOS Negl. Trop. Dis.* **13**, e0007462 (2019).
21. Shuai, L. et al. Immune responses in mice and pigs after oral vaccination with rabies virus vectored Nipah disease vaccines. *Vet. Microbiol.* **241**, 108549 (2020).
22. Foster, S. L. et al. A recombinant VSV-vectored vaccine rapidly protects nonhuman primates against lethal Nipah virus disease. *Proc. Natl. Acad. Sci. USA* **119**, e2200065119 (2022).
23. de Wit, E. et al. Distinct VSV-based Nipah virus vaccines expressing either glycoprotein G or fusion protein F provide homologous and heterologous protection in a nonhuman primate model. *EBioMedicine* **87**, 104405 (2023).
24. Muller, M. et al. Analysis of Nipah virus replication and host proteome response patterns in differentiated porcine airway epithelial cells cultured at the air-liquid interface. *Viruses* **15**, 961 (2023).
25. Abraham, M. et al. Evaluation of a new viral vaccine vector in mice and rhesus macaques: J paramyxovirus expressing hemagglutinin of influenza a virus H5N1. *J. Virol.* **95**, e0132121 (2021).
26. Beavis, A. C. et al. A J paramyxovirus-vectored HIV vaccine induces humoral and cellular responses in mice. *Vaccine* **42**, 2347–2356 (2024).
27. Xu, J. L. et al. Discovery and genetic characterization of novel paramyxoviruses from small mammals in Hubei Province, Central China. *Microb. Genom.* **10**, 001229 (2024).
28. DeRuyter, E., Subramaniam, K., Wisely, S. M., Jr., Morris, J. G. & Lednicky, J. A. A Novel Jeilongvirus from Florida, USA, has a broad host cell tropism including human and non-human primate cells. *Pathogens*. **13**, 831 (2024).
29. Findlay-Wilson, S. et al. Establishment of a Nipah virus disease model in hamsters, including a comparison of intranasal and intraperitoneal routes of challenge. *Pathogens*. **12**, 976 (2023).
30. Johnson, C. K. et al. Global shifts in mammalian population trends reveal key predictors of virus spillover risk. *Proc. Biol. Sci.* **287**, 20192736 (2020).
31. Chen, Z. et al. Evaluating a parainfluenza virus 5-based vaccine in a host with pre-existing immunity against parainfluenza virus 5. *PLoS ONE* **7**, e50144 (2012).
32. He, B., Paterson, R. G., Ward, C. D. & Lamb, R. A. Recovery of infectious SV5 from cloned DNA and expression of a foreign gene. *Virology* **237**, 249–260 (1997).

Acknowledgements

We appreciate the members of He laboratory for their helpful discussion and technical assistance.

Author contributions

Conceptualization and writing—original draft: E.W., and B.H.; formal analysis: E.W. and B.H.; investigation: E.W., J.P.S., C.P., S.R.W., E.K., M.C.G., A.G., Z.L., J.R.S., and B.H.; visualization: E.W. and B.H.; resources: B.H.; writing—review and editing: E.W. and B.H.; supervision: B.H. funding acquisition: B.H.

Competing interests

The University of Georgia has filed for a patent for the JPV vector system described in this work.

Additional information

Supplementary information The online version contains supplementary material available at https://doi.org/10.1038/s41541-025-01359-8.

Correspondence and requests for materials should be addressed to Biao He.